# Phase transitions in PZT-95/5 ceramics studied by dielectric and pyroelectric measurements: unusual properties in the vicinity of the antiferroelectric-ferroelectric phase transition



1995 J. Phys.: Condens. Matter 7 1721

(http://iopscience.iop.org/0953-8984/7/8/018)

J. Phys.: Condens. Matter 7 (1995) 1721–1728. Printed in the UK

# Phase transitions in PZT-95/5 ceramics studied by dielectric and pyroelectric measurements: unusual properties in the vicinity of the antiferroelectric–ferroelectric phase transition

J Hańderek and Z Ujma
Institute of Physics, University of Silesia, 40-007 Katowice, ul. Uniwersytecka 4, Poland

Received 10 October 1994

**Abstract.** The antiferroelectric–two ferroelectric ($F_{R(LT)}$–$F_{R(HT)}$)–paraelectric phase sequence was ascertained in PZT-95/5 ceramics. Unusual behaviour of the temperature characteristics of electric permittivity, tan $\delta$, remanent polarization and pyroelectric current was observed in the range of diffuse transition between the AFE and FE phases. The influence of external and internal bias electric fields as a possible reason for this behaviour is discussed.

## 1. Introduction

The vicinity of the phase boundaries separating the antiferroelectric (AFE) phase of orthorhombic symmetry ($A_O$ (Pbam)) and two ferroelectric (FE) phases of rhombohedral symmetry ($F_{R(LT)}$ (R3c) and $F_{R(HT)}$ (R3m)) in the phase diagram of PZT ceramics has long been the subject of considerable interest and intensive studies [1–13]. The specific properties exhibited by PZT ceramics with a [Zr]/[Ti] ratio close to 95/5 result from the marked influence of compositional fluctuations, intrinsic defects and admixtures on the local temperatures of phase transitions between these studied phases.

The properties of Nb- and La-doped PZT-95/5 ceramics have most often been investigated [3, 4, 11, 13–20]. Some of these investigations were reported in our recent papers [15–20]. More detailed description of the influence of the Nb and La dopants requires a comparison with data for 'pure' PZT-95/5 ceramics. An attempt to use earlier literature data and our previous experimental results [8, 12, 21–23] appeared deceptive owing to certain discrepancies in these data relating to the rather complex phase compositions of these ceramics. This indicated the necessity of repeating some previous measurements, paying special attention to the influence of the strength of measuring or previously applied electric field. Data on the unusual behaviour of the temperature characteristics of remanent polarization and pyroelectric current, obtained in various measuring conditions, especially with reference to the vicinity of the $A_O$–$F_R$ phase transition are reported in the present paper.

## 2. Dielectric measurements

The investigated PZT ceramics of composition $Pb(Zr_{0.95}Ti_{0.05})O_3$ were prepared using the conventional mixed-oxide method. The first thermal synthesis of blended and pressed PbO, $ZrO_2$ and $TiO_2$ was carried out at temperature of 950 °C for 3 h. The milled and cold-pressed

0953-8984/95/081721+08$19.50  

cylinders were then sintered twice at a temperature of 1100 °C and finally at 1250 °C for 3 h. These sintering processes were performed in a double crucible with a PbO atmosphere to maintain the established composition.

Samples of the required dimensions were coated with silver electrodes, using an appropriate paste not requiring thermal treatment. A sample of 0.6 mm thickness was used for measurements of electric permittivity $\varepsilon$ and dissipation factor (tan $\delta$) as a function of temperature. These measurements were performed at chosen frequencies of measuring field in the range 0.1–20 kHz, using a computerized automatic measuring system based on a Tesla BM-595 RLCG meter.

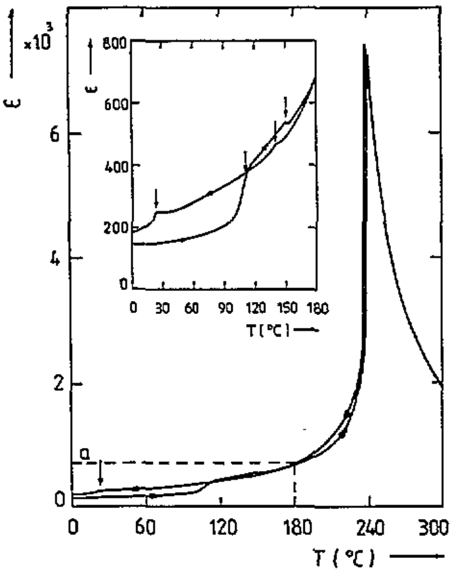


**Figure 1.** Temperature dependence of the permittivity, measured at a frequency of 1 kHz on heating (→) and cooling (←).

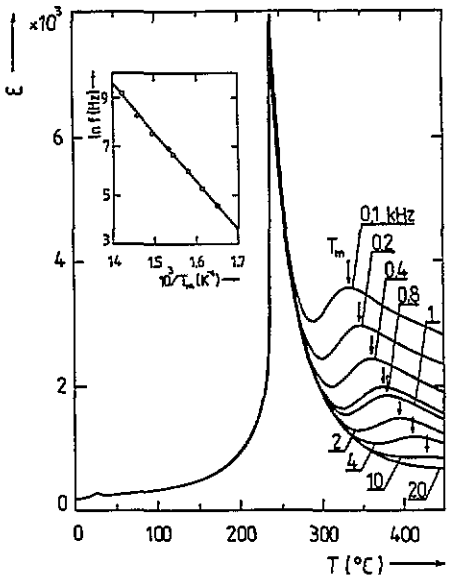


**Figure 2.** Temperature dependence of the permittivity, measured at chosen frequencies in the range 0.1–20 kHz on cooling and plot of ln $f$ versus $1/T_m$ (inset).

An example of $\varepsilon(T)$ curves, measured on heating and cooling, in a field frequency 1 kHz is shown in figure 1. Sharp maxima on the $\varepsilon(T)$ curves occur at the temperatures of the FE↔paraelectric (PE) phase transition (241 °C and 239 °C on heating and cooling, respectively). The distinct hump-like anomalies in the $\varepsilon(T)$ curves (indicated by arrows) occur at temperatures of about 110 °C and 24 °C on heating and cooling, respectively. These anomalies exhibit an exceptionally large thermal hysteresis on comparison of the heating and cooling processes. Some unusual properties, described below, were observed in the temperature range between these anomalies. Also noteworthy are additional small anomalies on the $\varepsilon(T)$ curve (figure 1, inset) at about 141 °C and 151 °C.

To obtain more precise data on the phase transitions and dielectric properties of these PZT-95/5 ceramics, measurements of $\varepsilon(T)$ and tan $\delta(T)$ were performed in a wide temperature range (0–500 °C) at various frequencies in the range from 0.1 to 20 kHz. As an example, $\varepsilon(T)$ curves measured on cooling are shown in figure 2. As may be seen, up to a temperature of about 260 °C the $\varepsilon(T)$ curves do not exhibit a distinct frequency dependence. At higher temperatures, in the PE range, additional broad anomalies (with maxima at $T_m$) in the $\varepsilon(T)$ curves occur, which are more distinct for lower frequencies and shift towards lower temperatures with decreasing frequency of the measuring field. The curve of natural logarithm of frequency $f$ versus the reciprocal absolute temperature $T_m$ (figure 2, inset) showed that the $f(T_m)$ dependence can be described by the well known Arrhenius formula $f = f_0 \exp(-E_a/kT_m)$, where the activation energy $E_a = 1.7$ eV and $f_0 = 2\times10^{16}$ Hz. The low-frequency dispersion occurring in the PE phase, observed also in the Nb- and La-doped PZT-95/5 ceramics, has been discussed in more detail in our previous papers [17–19].

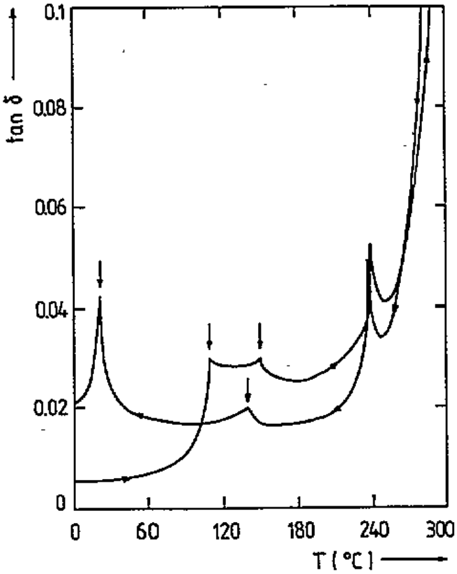


**Figure 3.** Temperature dependence of tan $\delta$, measured at a frequency of 1 kHz on heating (→) and cooling (←).

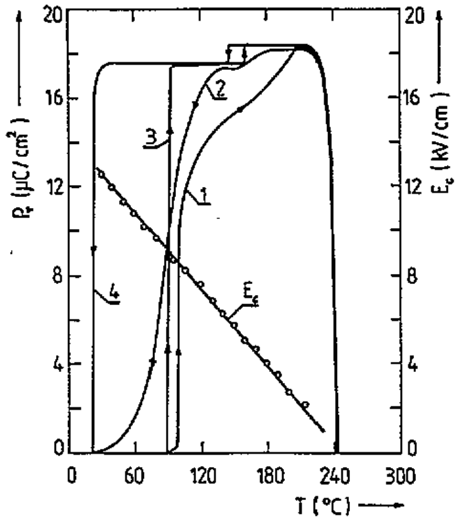


**Figure 4.** Remanent polarization obtained from hysteresis loop on heating (curves 1 and 3) and on cooling (curves 2 and 4) in a field of strength 10 kV cm$^{-1}$ (curves 1 and 2) and 20 kV cm$^{-1}$ (curves 3 and 4) and the coercive field $E_c$ as a function of temperature.

An example of tan $\delta(T)$ curves measured in a field of frequency 1 kHz is given in figure 3. It is worth noting the sharp local maxima in the tan $\delta(T)$ curves occurring at temperatures close to the FE↔PE phase transitions. Distinct anomalies in these curves occur also at temperatures at which hump-like anomalies in the $\varepsilon(T)$ curves were observed (figure 1). They also show the effect of the large thermal hysteresis, when comparing the heating and cooling processes. Additional distinct anomalies in the tan $\delta(T)$ curves occur at temperatures of about 150 °C and 140 °C on heating and cooling, respectively. These and the corresponding anomalies on the $\varepsilon(T)$ curves indicate an additional phase transition. Temperature variations in tan $\delta$ shown in figure 3 were also observed for other frequencies of the measuring field in the range from 0.1 to 20 kHz.

A sample of 0.3 mm thickness was used for the measurements of the hysteresis loops, in order to obtain remanent polarization $P_r$ versus temperature data. These measurements were performed in a field of frequency 50 Hz with various strengths of the measuring field. The $P_r(T)$ curves, measured on the heating–cooling cycles in fields of strengths 10 and 20 kV cm$^{-1}$, are shown in figure 4. The curve of coercive field $E_c$ versus temperature is also shown in this figure. A step-like increase in the $P_r(T)$ curves appeared during heating when passing through a temperature of about 90 °C (figure 4, curve 1). A steep decrease in $P_r$ occurs in the vicinity of the temperature of the FE→PE phase transition. The change in $P_r(T)$ on cooling through this temperature was also typical of the first-order FE↔PE phase transition. $P_r(T)$ variations of a very different type were observed on cooling in the temperature range from 140 to about 20 °C (curve 2), i.e. gradual decrease in $P_r$ when a measuring field of strength 10 kV $cm^{-1}$ was applied.

In a field of strength 20 kV $cm^{-1}$ (curves 3 and 4), relatively small jump-like changes in $P_r(T)$ were observed at temperatures of 160 °C and 145 °C on heating and cooling, respectively. Rapid disappearance of the hysteresis loop and $P_r$ occurs at a temperature of 20 °C. In a measuring field of strength 20 kV $cm^{-1}$ both phase transitions, at temperatures separating the FE state from the neighbouring PE and AFE phases, show the characteristics of first-order phase transitions. Anomalies in the $P_r(T)$ curves occurring in the vicinity of about 160 and 145 °C most probably correspond to the $F_{R(LT)}$–$F_{R(HT)}$ phase transition. There is a clear correlation between them and the corresponding anomalies on the $\varepsilon(T)$ and tan $\delta(T)$ curves (figures 1 and 3).

## 3. The measurements of pyroelectric and thermally stimulated depolarization currents

Prior to the pyroelectric measurements the PZT-95/5 sample was pre-polarized in a DC electric field of various strengths in the range 0.2–6 kV $cm^{-1}$, applied at a chosen temperature in the PE phase range, i.e. 250 °C, for 15 min and during subsequent cooling to 0 °C (i.e. below the FE→AFE phase transition). After the polarizing field has been switched off and the sample discharged by 1 min short-circuiting which allowed the depolarization current components with the shortest relaxation times to disappear the sample was then heated at a constant rate of 5 K $min^{-1}$. Between all the pre-poling and measuring cycles the sample was fully depolarized by thermal treatment at temperatures above 400 °C.

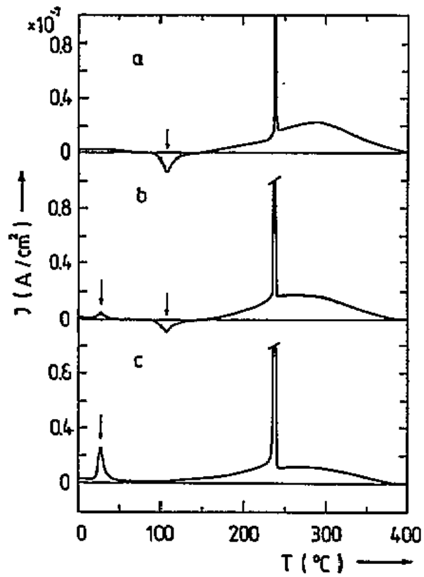


**Figure 5.** Pyroelectric current and TSDC recorded on heating for a sample pre-polarized in a field of strength (a) 1 kV $cm^{-1}$, (b) 2 kV $cm^{-1}$ and (c) 4 kV $cm^{-1}$.

Examples of pyroelectric current $I_p$ versus temperature, on the background of the thermally stimulated depolarization current (TSDC), recorded during subsequent heating are shown in figure 5 for the case when the pre-polarization procedures were finished at 0 °C. Typical variations in $I_p$ and TSDC for a sample pre-poled in a field of strength up to 1 kV cm$^{-1}$ are shown in figure 5(a). The broad peak on the $I_p(T)$ curve was first observed at 107 °C. This peak disappears at about 150 °C and then with increase in temperature the TSDC of opposite sign increases gradually. Next, a high and sharp peak of pyroelectric current occurs in the vicinity of the temperature of the FE–PE phase transition. A TSDC with a strongly broadened maximum was then observed in the range of the PE phase. It is noteworthy that it is precisely in this latter range that anomalies in $\varepsilon(T)$ curves (figure 2), showing low-frequency dispersion occur.

With a polarizing field of strength 1 kV cm$^{-1}$ < $E$ < 4 kV cm$^{-1}$ the behaviours of $I_p$ and TSDC were similar to those in the temperature range above 150 °C. In the temperature range below 150 °C, however, two broad peaks of opposite signs were observed in the $I_p(T)$ curves (figure 5(b)): the first at 107 °C, as in the foregoing case, and the second in the vicinity of 27 °C, i.e. approximately the temperatures at which corresponding changes in the $\varepsilon(T)$, tan $\delta(T)$ and $P_r(T)$ curves were observed on cooling. The sample pre-polarized in a field of strength 4 kV cm$^{-1}$ and higher shows only a peak at about 27 °C and the main peak of $I_p$ at the FE–PE phase transition. It is noteworthy that in all measurements performed in a polarizing field of strength $E$ < 4 kV cm$^{-1}$ the local change in the sign of measured current occurs at the same temperature, i.e. about 150 °C. This corresponds approximately to the anomalies on the $\varepsilon(T)$ (figure 1), tan $\delta(T)$ (figure 3) and $P_r(T)$ (figure 4) curves.

To elucidate the striking fact that the peak in pyroelectric current occurring in the vicinity of room temperature has the same sign as the peak at 240 °C (see figures 5(b) and 5(c)) the following experiment was performed. The previously depolarized sample was pre-poled again in fields of various strengths, applied also at 250 °C but switched off at 190 °C (i.e. inside the $F_{R(HT)}$ phase). After discharge and partial depolarization the sample was cooled at a rate of 5 K min$^{-1}$ to 0 °C. The behaviour of the TSDC and pyroelectric current versus temperature, for the case of a polarizing field $E$ of 0.4 kV cm$^{-1}$ is shown in figure 6(a). For comparison, the current on heating recorded earlier is also shown in this figure. The data in this figure indicate the clearly pyroelectric nature of both current peaks which are associated with the disappearance and appearance of $P_s$ on cooling and heating, respectively, through the AFE↔FE phase transitions.

Similar experiments were performed with a higher strength of polarizing field. Two examples, illustrating the behaviours of the pyroelectric current and TSDC versus temperature for cooling (the polarizing field switched off at 190 °C) and for heating (the polarizing field switched off at 0 °C) are shown in figures 6(b) and 6(c). Despite the peak in the pyroelectric current, occurring at about 107 °C, an additional peak in the vicinity of room temperature was observed on heating in a polarizing field of strength in the range 1 kV cm$^{-1}$ < $E$ < 4 kV cm$^{-1}$ (see the example in figure 6(b)). This latter peak has the same sign as the peak in pyroelectric current at the temperature of the FE–PE phase transition (see figure 5), while the first exhibits normal behaviour, corresponding to the appearance of $P_s$ at the AFE→FE phase transition. On cooling, only one of these peaks occurs, i.e. at a temperature of about 22 °C.

Even more unusual behaviour of the pyroelectric current was observed when the sample was pre-polarized in an electric field of strength 4 kV cm$^{-1}$ and higher (see example in figure 6(c)). In this case, only peaks in the vicinity of room temperature were observed on heating as well as on cooling. It is striking that the signs of current in these peaks are opposite to those corresponding to the appearance and disappearance of $P_s$ in the AFE→FE and FE→AFE phase transitions (figure 5). It is reasonable to suppose that the FE phase induced by an internal bias field of sufficient strength, associated with the space-charge polarization, should be taken into consideration for qualitative analysis of the unusual

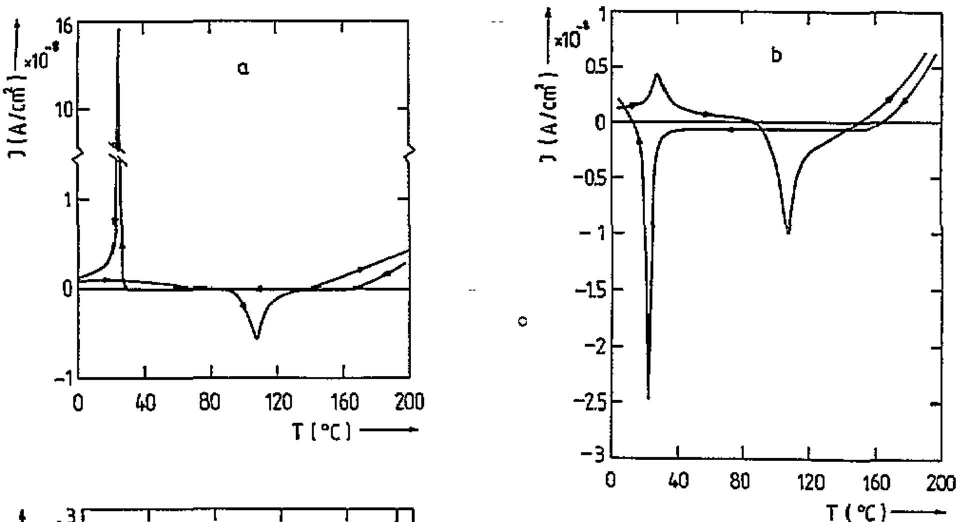


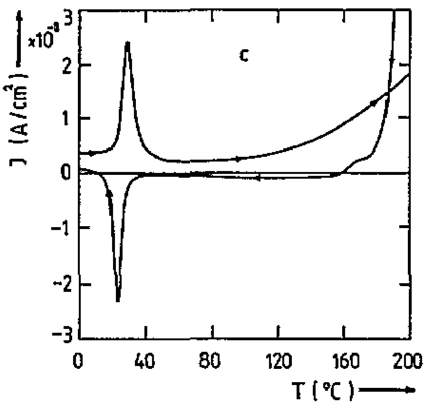


**Figure 6.** Pyroelectric current and TSDC recorded on heating (→) and cooling (←) for the sample pre-polarized in a field of strength (a) 0.4 kV $cm^{-1}$, (b) 2 kV $cm^{-1}$ and (c) 6 kV $cm^{-1}$.

behaviour of the pyroelectric current observed in the strongly pre-poled PZT-95/5 ceramic. The spontaneous polarization vector $P_s$ is in this case oriented opposite to that caused by the external polarizing field.

## 4. Discussion

The experimental data reported in the present paper showed an $A_O$–$F_{R(LT)}$–$F_{R(HT)}$–$P_C$ phase sequence in the investigated PZT-95/5 ceramics. On the basis of phenomenological theory, Haun *et al* [3] suggest that for the $PbZrO_3$–$PbTiO_3$ system a phase sequence of this kind also occurs in PZT ceramics with Ti content $0.03 < x < 0.05$, although this has been proved experimentally only in Zr-rich ceramics containing at least 6% Ti. Such a phase sequence was also considered by Wang *et al* [13] for the Nb-doped PZT-95/5 ceramics.

The specification of phase transition temperatures, obtained from the dielectric characteristics (figures 1–4) is given in table 1.

The most classical (normal) behaviour is that of the $F_{R(HT)}$–$P_C$ phase transition. This refers to the temperature characteristics of both dielectric and pyroelectric properties. The dielectric characteristics $\varepsilon(T)$, $\tan\delta(T)$ and $P_r(T)$, indicate the occurrence of two additional phase transitions at lower temperatures. The anomalies in these characteristics, observed in the temperature range 140–160 °C, are most probably associated with the $F_{R(LT)} \leftrightarrow F_{R(HT)}$

**Table 1.** Temperatures of phase transitions obtained from dielectric characteristics.

| | Temperature (°C) of the following phase transitions | | | | | |
|---|---|---|---|---|---|---|
| | $A_O$–$F_{R(LT)}$ | | $F_{R(LT)}$–$F_{R(HT)}$ | | $F_{R(HT)}$–$P_C$ | |
| Characteristic | Heating | Cooling | Heating | Cooling | Heating | Cooling |
| $\varepsilon(T)$ | 110 | 24 | 151 | 141 | 241 | 239 |
| $\tan\delta(T)$ | 109 | 22 | 150 | 140 | 239 | 237 |
| $P_r(T)$ | 88 | 20 | 160 | 145 | 243 | 241 |

phase transition. Our $P_r(T)$ measurements show, however, a decrease in $P_r$ during the presumed $F_{R(HT)} \rightarrow F_{R(LT)}$ phase transition, while an increase was ascertained in the case of PZT ceramics with higher Ti content [3, 24, 25]. No pyroelectric current associated with this phase transition was observed by us but a change in sign of measured current occurs at a temperature close to 160 °C (figures 5 and 6).

The most unusual is the behaviour of the pyroelectric current associated with the $A_O \leftrightarrow F_{R(LT)}$ phase transition. The dielectric characteristics studied also indicated other unusual features of this phase transition. One such is the exceptionally large thermal hysteresis effect, covering a temperature range of about 80 °C. The next such unusual feature is a marked shift in the average temperature of the $F_{R(LT)}$–$A_O$ phase transition under the influence of the applied electric field, ascertained in our earlier papers [12, 22]. The gradual shift in this temperature was observed with increase in strength of the applied DC or AC electric field, in contrast with the effect of the shift in the $F_{R(LT)}$–$A_O$ phase transition temperature in the strongly pre-polarized sample (figures 5(b), 5(c), 6(b) and 6(c)).

To gain an insight into the unusual behaviour of the pyroelectric current observed in the strongly pre-polarized PZT-95/5 ceramics requires taking into consideration the complex phase composition in the temperature range in the vicinity of the average temperature of the $A_O$–$F_{R(LT)}$ phase transition and also the presence of space-charge polarization and associated internal bias electric field in the pre-polarized sample. Our earlier and recent x-ray measurements indicated the coexistence of the $A_O$ and $F_R$ phases, particularly in PZT ceramics with a Ti content $0.03 < x < 0.08$ [12, 23, 26]. The coexistence of these phases in the individual grains was also ascertained in the PZT-95/5 ceramics by TEM studies [14]. The exceptionally strong diffuse character of the $A_O \leftrightarrow F_R$ phase transition is caused by the different local phase transition temperatures, which are due to compositional fluctuations in the concentrations of Pb, Zr and Ti ions, vacancies in the Pb and O sublattices, local internal electric fields and mechanical stresses. The remaining FE domains in the AFE matrix are additionally stabilized by screening of $P_s$ by the ionic and electronic charges from the surrounding space and from the electrodes. The spontaneous polarization of such domains is not reversible and does not give rise to remanent polarization, at least in the case of a weak electric field applied during measurements of the hysteresis loop (figure 4, curves 1 and 2). A sufficiently strong field causes the release of electronic charges participating in the screening process, giving in effect an increase in the $P_r$-value (figure 4, curves 3 and 4). It is noteworthy that in the latter case the $P_r(T)$ curves on heating (figure 4, curves 1 and 3) show an $A_O$–$F_{R(LT)}$ phase transition at about 90 °C. Therefore it is reasonable to conclude that the appearance of the peak in the pyroelectric current in the vicinity of 20 °C in the strongly pre-polarized sample (Figures 5(b), 5(c), 6(b) and 6(c)) is induced by the internal bias electric field, associated with the macroscopic space-charge polarization occurring during the pre-polarization procedure. The migration of mobile ionic defects under the applied polarizing field and their accumulation in the surface layers give rise to different properties between the surface layers and the bulk of the ceramic sample. Consequently, the local phase transition temperatures, phase composition and many other properties in these parts of the sample are changed. This could explain the origin of the two peaks in the pyroelectric current, occurring on heating in the vicinity of 27 °C and 107 °C in the sample pre-polarized in a field of strength 1 kV $cm^{-1}$ $< E <$ 4 kV $cm^{-1}$ (figures 5(b) and 6(b)). In the case of the more strongly pre-polarized sample (figures 5(c) and 6(c)) the induced $F_{R(LT)}$ phase predominates throughout the whole sample volume. Reasoning from this point of view, it could be expected that conditions of such strong pre-polarization depend on sample thickness.

It is worth stressing that the PZT-95/5 ceramics tested exhibit high-frequency dielectric dispersion in the gigahertz range [27, 28]. Rapid response of these ceramics to the application of short high-voltage impulses and both electric and laser light impulses was also ascertained during investigations of strong electron emission from PZT ceramics with a [Zr]/[Ti] ratio of 95/5 [29–32]. This exceptionally fast response results either from $P_s$ switching in the twin FE domains existing in these ceramics [14] and/or the discussed fast transformation of the metastable $A_O$ phase to $F_{R(LT)}$ in the temperature range from 20 to 110 °C, which can be induced by sufficiently strong external or internal bias electric field.

## References


[1] Sawaguchi E 1953 *J. Phys. Soc. Japan* **8** 615
[2] Jaffe B, Cook W R and Jaffe H 1971 *Piezoelectric Ceramics* (London: Academic)
[3] Haun M I, Halemane R T, Newnham R E and Cross L E 1985 *Proc. 6th IMF, (Kobe 1985) Japan. J. Appl. Phys.* **24** Suppl. 2 209–11
[4] Haertling G H and Land C E 1971 *J. Am. Ceram. Soc.* **54** 1
[5] Haertling G W 1987 *Ferroelectrics* **75** 25
[6] Haertling G W 1991 *Ceramic Materials for Electronics* ed R C Buchanan (New York: Buchanan) ch 3
[7] Berlincourt D, Krueger H H A and Jaffe B 1964 *J. Phys. Chem. Solids* **25** 659
[8] Hańderek J and Ujma Z 1977 *Acta Phys. Pol.* A **51** 87
[9] Morozov E M 1977 *Fiz. Tverd. Teta.* **7** 42
[10] Whatmore R W, Clarke R and Glazer A M 1978 *J. Phys. C: Solid State Phys.* **11** 3089
[11] Fritz I J and Keck I D 1978 *J. Phys. Chem. Solids* **39** 1163
[12] Hańderek J, Kwapuliński J, Ujma Z and Roleder K 1988 *Ferroelectrics* **81** 253
[13] Wang Y L, Cheng Z M, Sun Y R and Dai X H 1988 *Physics* B **150** 168
[14] Chang Y I 1982 *Appl. Phys.* A **29** 237
[15] Hafid M, Hańderek J, Kugel G E and Fontana M D 1992 *Ferroelectrics* **125** 477
[16] Carabatos-Nedélec C, Harrad I El, Hańderek J, Bréhat F and Wyncke B 1992 *Ferroelectrics* **125** 483
[17] Hafid M, Kugel G E, Hańderek J and Ujma Z 1992 *Ferroelectrics* **135** 101
[18] Kugel G, Hafid M, Hańderek J, Ujma Z and Dmytrów D 1992 *Ferroelectrics* **133** 121
[19] Hańderek J, Ujma Z, Carabatos-Nedélec C, Kugel G E, Dmytrów D and El Harrad I 1993 *J. Appl. Phys.* **73** 367
[20] El Harrad I, Carabatos-Nédelec C, Hańderek J, Ujma Z and Dmytrów D 1994 *J. Raman Spectrosc.* **25** 799
[21] Hańderek J, Ujma Z and Roleder K 1980 *Phase Transitions* **1** 377
[22] Roleder K and Hańderek J 1982 *Phase Transitions* **2** 285
[23] Hańderek J, Kwapulinski J, Pawełczyk M and Ujma Z 1985 *Phase Transitions* **6** 35
[24] Clarke R and Whatmore R W 1976 *J. Cryst. Growth* **33** 525
[25] Clarke R, Glazer A M, Aiger F W, Appleby D, Poole N J and Porter S G 1976 *Ferroelectrics* **11** 359
[26] Ujma Z, Hańderek J, Pawełczyk M, Hassan H, Kugel E G and Carabatos-Nédelec C 1994 *J. Phys.: Condens. Matter* **6** 6843
[27] Shaoping L, Sheen J, Jang S J, Bhalla A B and Cross L E 1993 *Ferroelectrics Lett.* **16** 21
[28] Hassan H, Maglione M, Fontana M D and Hańderek J 1994 *J. Phys.: Condens. Matter* submitted
[29] Gundel H, Riege H, Wilson E I N, Hańderek J and Zioutas H 1989 *Ferroelectrics* **100** 1
[30] Gundel H, Hańderek J, Riege H, Wilson E I N and Zioutas H 1990 *Ferroelectrics* **109** 137
[31] Gundel H, Hańderek J and Riege H 1991 *J. Appl. Phys.* **69** 975
[32] Geissler K, Meineke A, Riege H, Schmidt K and Hańderek J 1993 *Phys. Lett.* **176A** 387